RESEARCH PAPER

Preparation and Characterization of ZnO Nanoparticles Using the Hydrothermal method Technique with Evaluation of Antibacterial Properties

*Ghufran K. Ibadi [1], Shaymaa Omar Mohammed [1], Aymen Wasfi Dhahir [2], Noor Malik Saadoon [3,4] **

[1] College of Biomedical Engineering, University of Technology, Iraq

[2] Department of Healthy Physic and Radiation Therapy Engineering Technique, Alsharq College of Specialized Technical Science, Iraq

[3] Nanotechnology and Advanced Materials Research Center, University of Technology, Baghdad, Iraq

[4] College of Biomedical Engineering, University of Technology, Iraq

ARTICLE INFO

Article History:
Received 11 December 2025
Accepted 26 March 2026
Published 01 April 2026

Keywords:
Nano-sized agglomerates
Nanoparticles
X-ray (XRD)
Zinc oxide

ABSTRACT

The article describes the sol-gel process used to construct and assess ZnO nanoparticles. This method is noted for producing ZnO nanomaterials with controlled dimensions and morphologies. ZnO NP have been confirmed to have a quartzite structure (approximately 30 nm crystallite size) through X-ray crystallographic analyses. Dynamic light scattering techniques measured an average hydrodynamic particle radius of approximately 70 nm; therefore, there is some degree of agglomeration calculated. SEM provides further verification of this report; once again, displaying components of polymorphically aggregated, nanosized ZnO NPs. Although the whole particle system aggregates uniformly, the possible effect of the aggregate behaviour of ZnO on the properties and potential application areas (i.e., catalysis, photovoltaics, and sensing technologies). In addition to demonstrating effective use of the sol-gel process for producing ZnO NP's of controlled dimensions, the following study provides valuable information about their tendency toward aggregation. These data are necessary to optimize the performance of these materials in a variety of applications.

How to cite this article
Ibadi G., Mohamme S., Dhahir A., Saadoon N. Preparation and Characterization of ZnO Nanoparticles Using the Hydrothermal method Technique with Evaluation of Antibacterial Properties. J Nanostruct, 2026; 16(2):2041-2049. DOI: 10.22052/JNS.2026.02.050

INTRODUCTION

The rapid advancement of nanotechnology enables the rational design and synthesis of functional nanomaterials with tailored physicochemical characteristics for intended applications. Zinc oxide (ZnO) nanoparticles, in particular, have received a great deal of interest, because of their semiconducting nature, high exciton binding energy, wide band gap (~3.37 eV). These qualities make ZnO nanoparticles highly suitable for applications across the fields of optoelectronics, catalysis and biomedicine. The increasing number of studies investigating the production of nanostructured ZnO materials continues to grow [1-3].

Due to its low cost, short luminescence time,

* *Corresponding Author Email: mae.visit.04@uotechnology.edu.iq*

and wavelength (550 nm), zinc oxide (ZnO) is used in a wide variety of devices, including unipolar transistors and LEDs [4]. In terms of their crystal structure, nanostructured materials based on ZnO are of particular interest. These materials can be used as gas sensors [5], piezoelectric devices, photovoltaic cells, and solar batteries [6]. Hollow microspheres and flower-like shapes of ZnO can all be formed into three-dimensional structures [7]. Interestingly, the flower-like structures of ZnO are composed of networks of nanorods and nanosheets. In addition, three-dimensional ZnO nano flowers are considered as possible candidates for use as gas sensors [8] due to their large specific surface area and high room temperature sensitivity. Additionally, ZnO Nano flowers have found a purpose in tissue engineering in the medical world [9]. With the growing number of multi-drug resistant (MDR) bacteria around, it has become imperative for health systems worldwide to come up with new methods of fighting bacteria, other than what we now use (the standard antibiotics).

Metal oxide (particularly zinc oxide: ZnO) nanoparticles present a unique opportunity due to their multidimensional mechanism of action against bacteria and low incidence of developing resistant bacteria. While traditional antibiotics target specific biochemical pathways, the antimicrobial activity of ZnO nanoparticles occurs through multiple and diverse means. The antibacterial activity of ZnO nanoparticles also relates directly to their ability to produce Reactive Oxygen Species (ROS) when irradiated with UV light, and when illuminated with visible light through the formation of electron–hole pairs. Finally, as ZnO dissolves into solution, the release of Zn^{2+} ions disrupts enzymes that are intracellularly located and disrupts membrane integrity. Other properties of the ZnO nanoparticles, such as surface defects, oxygen vacancies, and particle morphology all influence the activity of these nanoparticles at the Nano–bio interface. The chemical reduction technique is one of the many methods for synthesising ZnO nanoparticles. It has a high degree of robustness and scalability and can produce ZnO nanoparticles having controllable morphology and narrow particle size distributions. Furthermore, the chemical reduction method permits the fine-tuning of the kinetics associated with both the nucleation of the nanoparticles and the growth of the nanoparticles by varying the various parameter(s) associated with the reaction, including the precursor concentration, pH, temperature, and the type(s) of capping agent(s) utilized.

MATERIALS AND METHODS

Synthesis of ZnO Nanoparticles

The first step consisted of a preparation of the zinc sulphate solution $ZnSO_4.7H_2O$ (0.015 M). The second step was to add sodium bicarbonate solution (0.04 M). The addition of sodium bicarbonate solution to the zinc sulphate solution at a rate of one drop per drop was accomplished using a magnetic stirrer to ensure thorough mixing. Once the solution appeared cloudy, zinc hydroxide was produced as a precipitate. The precipitate was then washed three times with distilled water. The precipitate subsequently was heated in an oven for 80°C for three hours. Finally, the resultant nano sized zinc oxide was produced by heating at 350°C for three hours in a muffle oven. Resultant product was a white powder.

RESULTS AND DISCUSSION

Characterization of ZnO nanoparticles with X-ray diffraction (XRD)

To confirm the synthesis of phase-pure Zinc Oxide nanoparticles, the crystallinity and purity of the obtained nanoparticles were assessed using X-ray diffraction (XRD) with Cu Kα radiation (λ = 1.5406 Å). The XRD patterns illustrate multiple well-defined peaks found at the following 2θ values; ~31.7°, ~34.4°, ~36.2°, ~47.5°, ~56.6°, ~62.8°, ~66.3°, ~67.9° and ~69.1° which correspond to the (100), (002), (101), (102), (110), (103), (200), (112) and (201) crystalline planes, respectively (shown in Figs. 1 and 2). These plane reflections were found to be in excellent agreement with the standard hexagonal wurtzite crystalline structure of ZnO, provided by the JCPDS card number 36-1451; therefore further confirming that a phase-pure synthesis of ZnO was completed. The entirety of the identified peaks (i.e. reflection peaks) demonstrate no additional impurities such as; either $Zn(OH)_2$ or any other Zn compound, are present within the detection limits of the instrument. The sharp, well-resolved diffraction (i.e. intensity) peaks observed in the XRD patterns were indicative of highly crystalline materials. There is some minor broadening of the peaks observed, indicating that these materials are in the size range of “nano,” and may also have

a finite amount of crystallite size (i.e. crystallite size is variable) and possibly some microstrains in the lattices. Table 1 shows that the peak intensity is greater for the (002) plane versus the other planes, which indicates that the majority of crystal growths take place along the c-axis of the hexagonal crystal structure. Anisotropic crystallite growth behaviour in ZnO nanostructures results from the wurtzite crystal structure having polar characteristics. [12-14].

Scanning Electron Microscopy (SEM) Analysis

Using scanning electron microscopy (SEM), the morphologic and microstructural characteristics of the synthesized Zinc Oxide nanoparticles were evaluated. The SEM image shows that this sample has many different types of densely agglomerated nanostructures found on a microscopic surface. These particles also have a variety of shapes: most are quasi-spherical nanoparticles; some are short, rod-shaped and/or irregular granular structures. The primary particles, when viewed at 20,000X, may appear to be in the nano range; however, because they have such high surface energy and high levels of attraction between them; they tend to combine into large secondary aggregates. This is a typical feature of all ZnO nanoparticles, as shown in Fig. 2.

The synthesized ZnO shows clusters of particles that have a looser arrangement and more open spaces between them, which may maximize the surface area of the material. Additionally, there

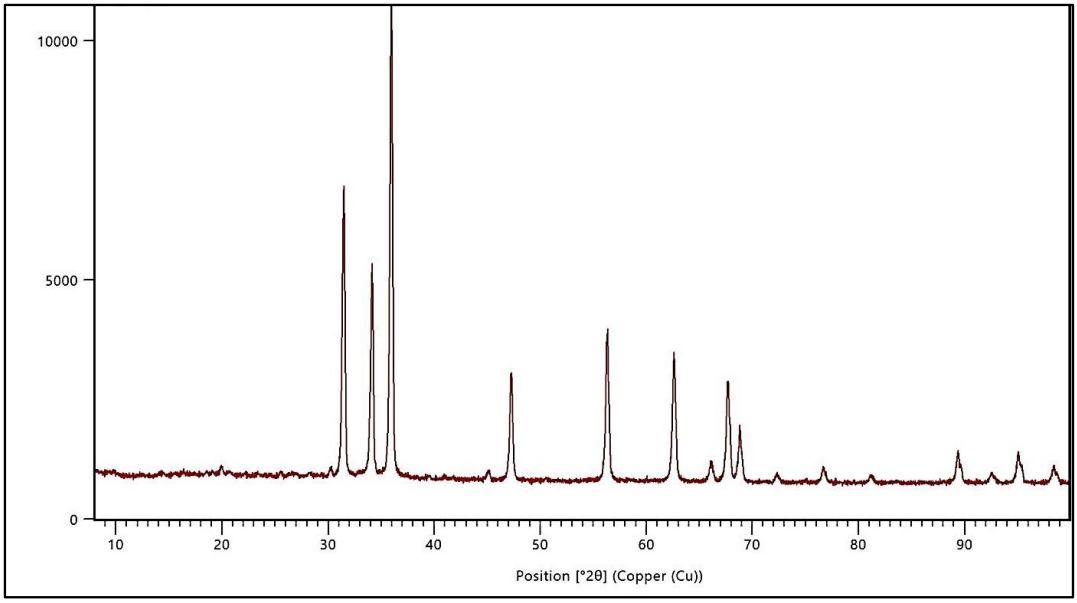

Fig. 1. X-ray diffraction of a zinc oxide.

Table 1. XRD Peak Table for ZnO NPs.

2θ (degree)	Intensity	Miller Indices (hkl)
31.7	Strong	100
34.4	Very strong	002
36.2	Strong	101
47.5	Medium	102
56.6	Medium	110
62.8	Medium	103
68.66	Weak	200
77.72	Weak	112

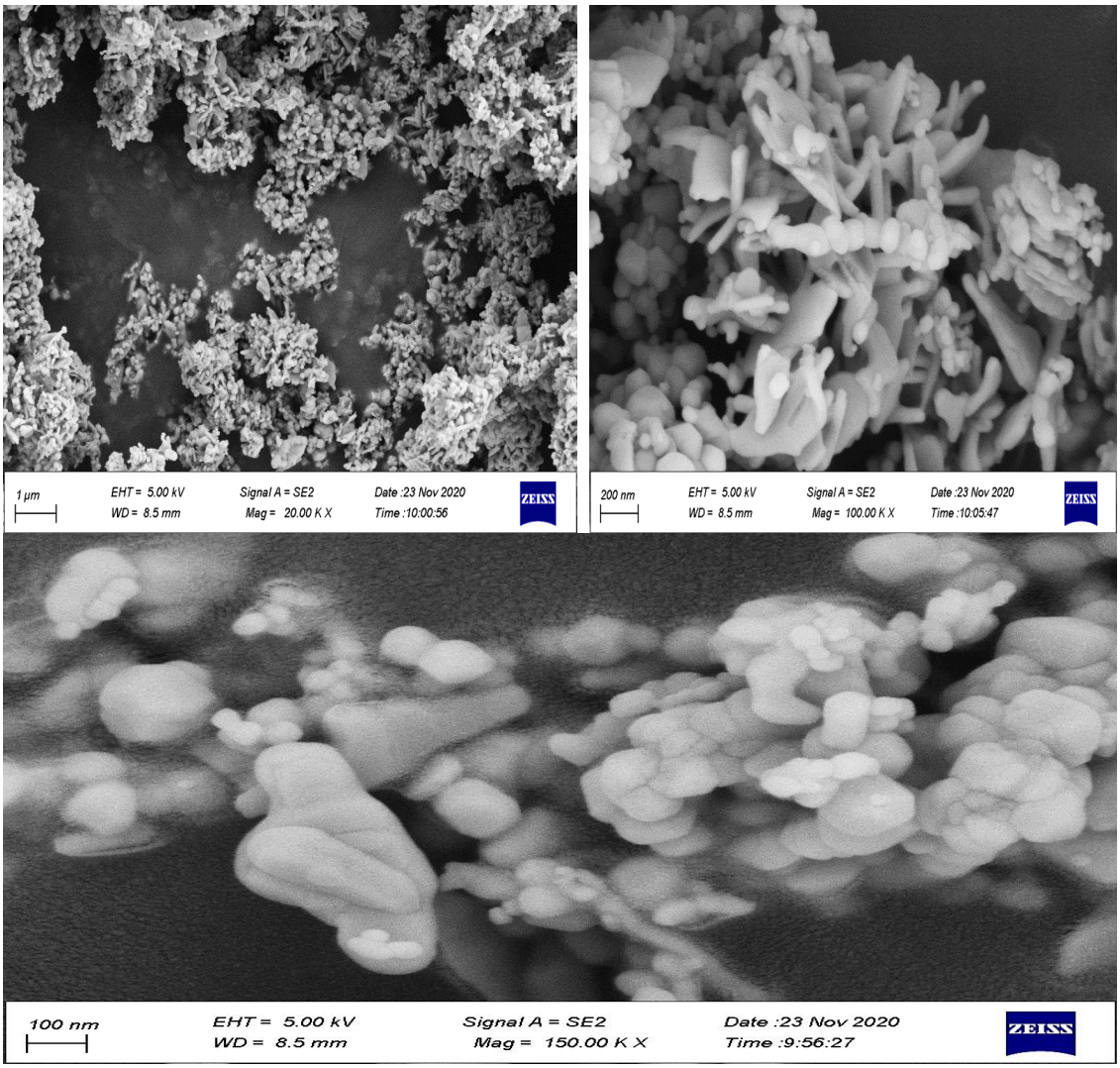

Fig. 2. Scanning Electron Microscopy (SEM) for ZnNPs.

Fig. 2. Scanning Electron Microscopy (SEM) for ZnNPs.

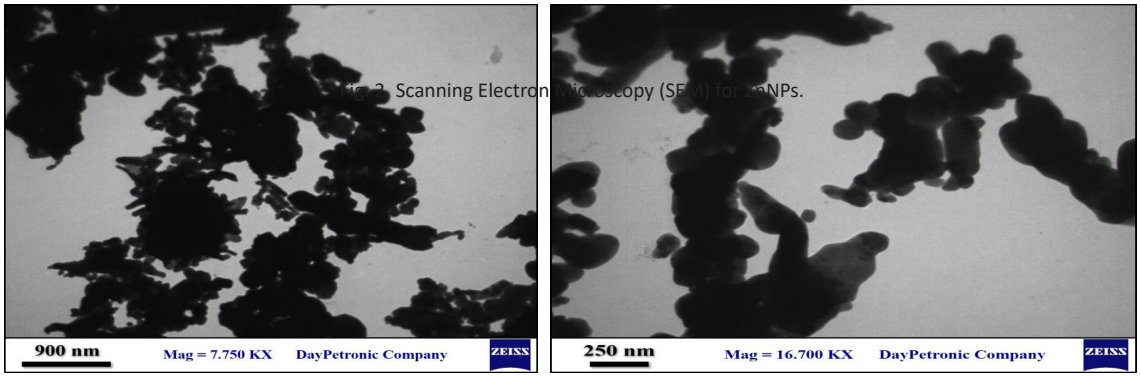

Fig. 3. TEM for ZnO NPs.

exist mixed morphologies (e.g., rods) indicating that growth occurs preferentially in specific crystallographic directions, consistent with the preferential growth along the (002) crystal plane indicated by the XRD results. Therefore, it is reasonable to conclude that the growth of ZnO nanocrystals is related to the inherent polarity of the hexagonal wurtzite crystal lattice structure. In general, the SEM images indicate that the synthesized ZnO consists of agglomerated porous forms of nanoscale primary particles with mixed morphologies, providing further evidence of its high degree of crystallinity and nanoscale character identified in the XRD findings [15].

Morphological and Surface Analysis (TEM and AFM)

The morphology and surface characteristics of the sample prepared were studied by using Transmission Electron Microscopy (TEM) and

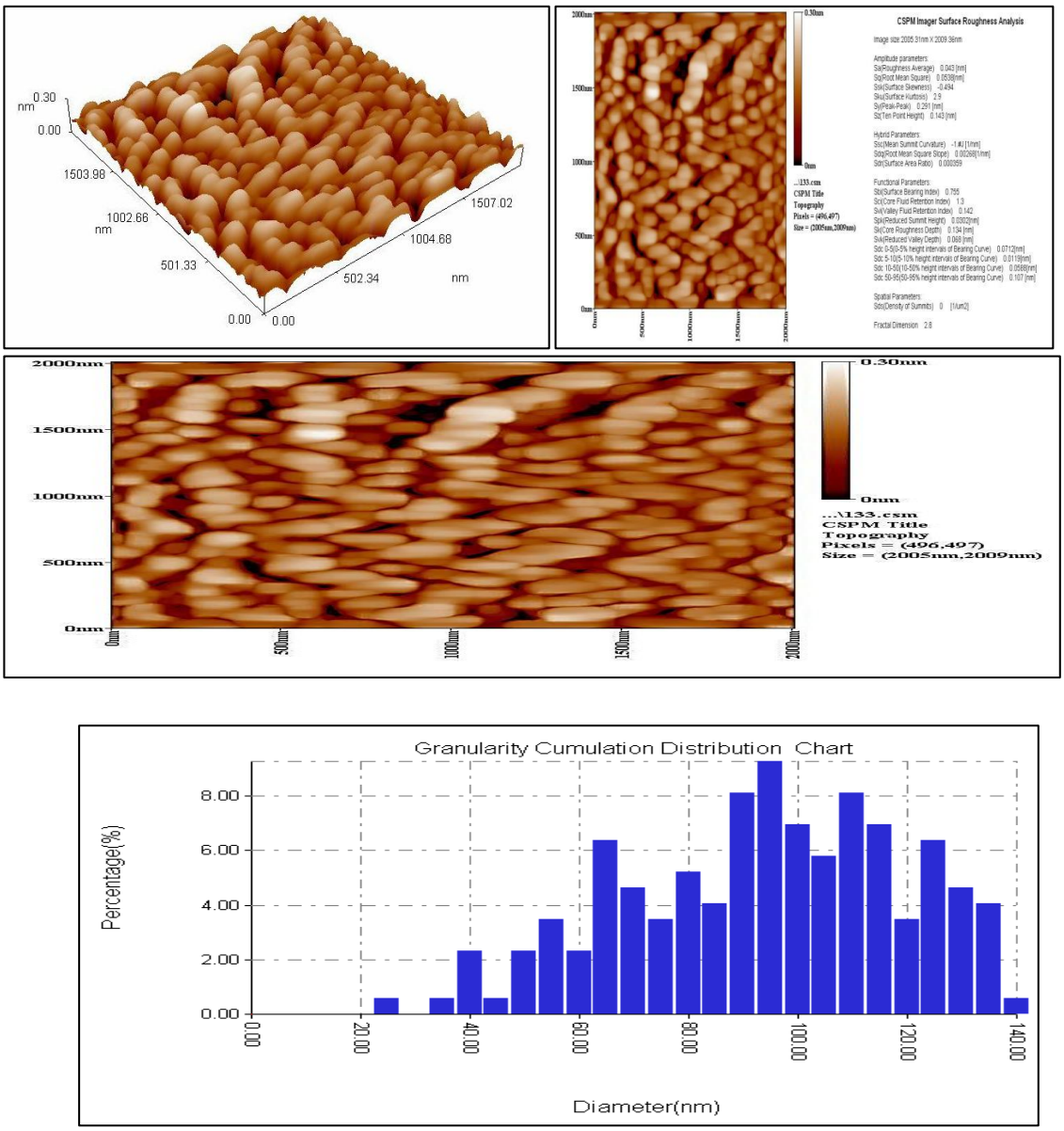

Fig. 4. AFM image for ZnO nanoparticles.

Atomic Force Microscopy (AFM) as complementary methods of determining the particle structure and surface topology. In the TEM image, the nanostructures present are shown to be irregularly shaped and there is evidence that these nanoparticles have formed highly agglomerated clusters (Fig. 3). Within the TEM image, the nanoparticle clusters are shown as areas of dark contrast, which indicates that the material has a high electron density. TEM also shows the agglomeration of the nanoparticle clusters as chain-type and island-type forms, and the nanoparticle agglomerates range from submicron to micron size; however, the primary particle size is much smaller than the agglomerates and it is difficult to distinguish the primary particles as a result of extreme agglomeration. By analyzing the AFM, we have learned a lot about the sample's surface topography/roughness. Scans of the sample (Fig. 4, 2D images, and 2D images, 2.0 x 2.0 µm sq. areas), have shown a very normally distributed/ exclusively packed granular morphology. There are nano-dome-type features that are arranged very closely to each other without any significant voids or cracks indicating high levels of uniformity/ continuity. Quantitative roughness measurements indicate that the surface is relatively smooth with variations at a nanoscale level. The average surface roughness (Sa) is approximately 0.043 nm and root mean square roughness (Sq) equals approximately 0.0630 nm. This data shows that a low-roughness and highly compact Surface has been developed on the sample. A negative skewness (Ssk) value (≈ -0.494) indicates that the surface consists mainly of shallow valleys, while the kurtosis (Sku) (≈ 2.9) indicates that the heights of the structures on the surface are nearly normally distributed. Together the above quantitative results show that the

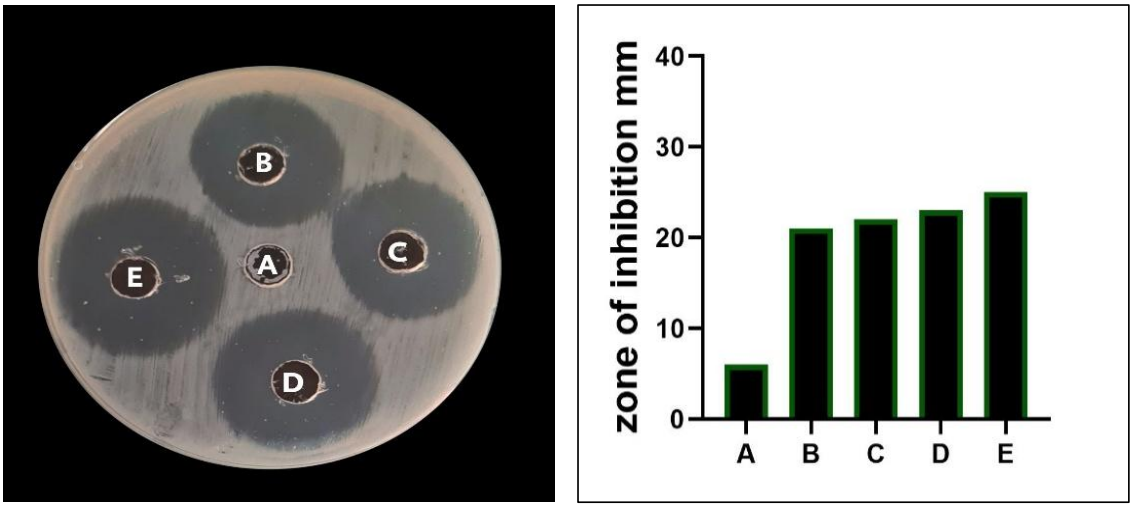

Fig. 5. Antibacterial activity of (Plant extract) against *S.aureus.* A, (DIW). B, 62.5 µg/mL. C, 125 µg/mL. D, 250 µg/mL. E, 500 µg/mL.

Table 2. Explain the antibacterial activity of nanoparticles.

Antibacterial analysis(Zone of inhibition (mm)					
Sample	A	B	C	D	E
S.aureus	6	21	22	23	25
E.coli	6	23	32	35	37

surface is highly homogenous and well-organized. Images captured using AFM reveal characteristics of slight elongation and anisotropic or grain forms which range from tens of nanometers to a few hundred nanometres in their lateral dimensions and were likely caused by particle coalescence during the process of manufacturing the film [17-18].

Prepare of Mueller Hinton agar

Muller-Hinton (M-H) prepared by adding 38 g of the powder into 1 L distilled water and then heated on a burner with shaking. M-H must be autoclaved for 15 minutes at 121°C to be sterilized. Then it was allowed to cool to 50°C before pouring into a petri dish and leaving for about 15 minutes for solidification before flipping upside down and storing in the refrigerator at 4°C.

Antibacterial activity

ZnO-NPs were tested for antibacterial potential using an agar well diffusion assay against both Gram-positive and Gram-negative bacteria. To accomplish this, approximately 20 mL of MH agar was poured into sterile petri dishes using aseptic technique. Using a sterile wire loop, the bacterial strains were picked from their respective stock cultures. Following the proper incubation period for the bacteria, 6 mm holes were created in the agar plates with the use of a sterile tip. Different concentrations of ZnO-NPs were then placed into each of the holes in the agar plates. The agar plates containing the ZnO-NPs and the bacteria were incubated overnight at 37°C prior to recording the average size of the zone of inhibition for each of the different concentrations of ZnO-NPs.

Result of Antibacterial activity

The success of synthesizing ZnO nanoparticles is demonstrated by the formation of a white powder that corresponds to the successful formation of the ZnO phase. The potential for a higher level of bactericidal activity than standard ZnO can be explained by several interrelated mechanisms. First, ZnO nanoparticles produce reactive oxygen species (ROS) such as hydroxyl radicals (•OH), superoxide radicals (O_2^-) and hydrogen peroxide (H_2O_2) causing oxidative damage to the bacterial cell; this includes lipid peroxidation, protein denaturation, and DNA damage. Second, ZnO nanoparticles also release Zn^{2+} ions (when in solution) that can diffuse across the bacterial cell membrane leading to the loss of the ion's ability to maintain cellular metabolic homeostasis. [23]. Further, the electrostatic attraction of the positively charged nanoparticle and negatively charged bacterial membrane increases the permeability of the membrane, resulting in cytoplasmic leakage. Additionally, nanoparticle size, morphology and surface defect density have a significant impact on the ability of the nanoparticle to exhibit antibacterial activity. More

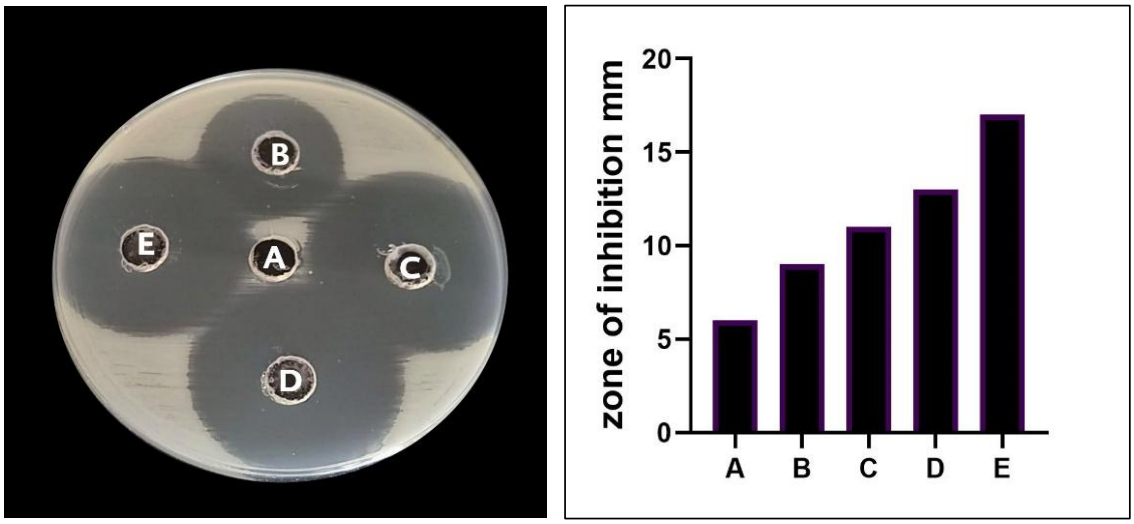

Fig. 6. Antibacterial activity of (sample 2) against *Ecoli* A, Control. B, 62.5 µg/mL. C, 125 µg/mL. D, 250 µg/mL. E, 500 µg/mL.

toxic reactivity and high capacity for generating reactive oxygen species (ROS), view Table 2. As such, all data associated with the antibacterial activity for different concentrations as illustrated by these Figs. 5 and 6.

CONCLUSION

The results obtained from this study indicate the ability to manufacture ZnO nanoparticles using a controlled hydrothermal approach. It was shown that they have significant antibacterial activity against Gram-positive and Gram-negative bacteria. It is thought that the antimicrobial effect of ZnO nanoparticles derives from several combined physicochemical and biochemical activities such as reactive oxygen species (ROS) production, ion release (dissolution), and disruption of membranes. Thus, at the 'mechanistic' level, ZnO nanoparticles demonstrate multiple mechanisms of action against microorganisms (bacteria), and therefore, because of their various modes of action, there is little chance that resistance will develop to this type of material; thus, ZnO nanoparticles represent a viable option as a next-generation antimicrobial. There are still many questions left unanswered by this study; therefore, future studies must be done using in vivo methods, evaluating cytotoxicity, modifying the surface of the nanoparticles to enhance selectivity and biocompatibility.

CONFLICT OF INTEREST

The authors declare that there is no conflict of interests regarding the publication of this manuscript.

REFERENCES

1. Sengani M, Grumezescu AM, Rajeswari VD. Recent trends and methodologies in gold nanoparticle synthesis – A prospective review on drug delivery aspect. OpenNano. 2017;2:37-46.
2. Herizchi R, Abbasi E, Milani M, Akbarzadeh A. Current methods for synthesis of gold nanoparticles. Artificial Cells, Nanomedicine, and Biotechnology. 2014;44(2):596-602.
3. Gharawi MA, Saadoon AM, Hmoad NR, Albayati AH. Structural performance of rail connections: Experimental testing and finite element modeling. Results in Engineering. 2025;27:105997.
4. Mohazzab BF, Jaleh B, Nasrollahzadeh M, Issaabadi Z, Varma RS. Laser ablation-assisted synthesis of GO/TiO_2/Au nanocomposite: Applications in K3[Fe(CN)6] and Nigrosin reduction. Molecular Catalysis. 2019;473:110401.
5. Staudinger U, Janke A, Simon F, Jakisch L, Bittrich E, Formanek P, et al. MWCNT Localization and Electrical Percolation in Thin Films of Semifluorinated PMMA Block Copolymers. Polymers. 2025;17(9):1271.
6. Nancy P, Nair AK, Antoine R, Thomas S, Kalarikkal N. In Situ Decoration of Gold Nanoparticles on Graphene Oxide via Nanosecond Laser Ablation for Remarkable Chemical Sensing and Catalysis. Nanomaterials. 2019;9(9):1201.
7. Hernández-Maya M, Rivera-Quintero P, Ospina R, Quintero-Orozco JH, García-Castro AC. Ablation energy, water volume and ablation time: Gold nanoparticles obtained through by pulsed laser ablation in liquid. Journal of Physics: Conference Series. 2019;1386(1):012062.
8. Alluhaybi HA, Ghoshal SK, Shamsuri WNW, Alsobhi BO, Salim AA, Krishnan G. Pulsed laser ablation in liquid assisted growth of gold nanoparticles: Evaluation of structural and optical features. Nano-Structures and Nano-Objects. 2019;19:100355.
9. Size and Chemistry Controlled Cobalt-Ferrite Nanoparticles and Their Anti-proliferative Effect against the MCF7 Breast Cancer Cells. American Chemical Society (ACS). http://dx.doi.org/10.1021/acsbiomaterials.6b00333.s001
10. Letzel A, Gökce B, Menzel A, Plech A, Barcikowski S. Primary particle diameter differentiation and bimodality identification by five analytical methods using gold nanoparticle size distributions synthesized by pulsed laser ablation in liquids. Appl Surf Sci. 2018;435:743-751.
11. Naharuddin NZA, Sadrolhosseini AR, Abu Bakar MH, Tamchek N, Mahdi MA. Laser ablation synthesis of gold nanoparticles in tetrahydrofuran. Optical Materials Express. 2020;10(2):323.
12. Bailly A-L, Correard F, Popov A, Tselikov G, Chaspoul F, Appay R, et al. In vivo evaluation of safety, biodistribution and pharmacokinetics of laser-synthesized gold nanoparticles. Sci Rep. 2019;9(1).
13. Daruich De Souza C, Ribeiro Nogueira B, Rostelato MECM. Review of the methodologies used in the synthesis gold nanoparticles by chemical reduction. J Alloys Compd. 2019;798:714-740.
14. Riedel R, Mahr N, Yao C, Wu A, Yang F, Hampp N. Synthesis of gold–silica core–shell nanoparticles by pulsed laser ablation in liquid and their physico-chemical properties towards photothermal cancer therapy. Nanoscale. 2020;12(5):3007-3018.
15. Kong F-Y, Zhang J-W, Li R-F, Wang Z-X, Wang W-J, Wang W. Unique Roles of Gold Nanoparticles in Drug Delivery, Targeting and Imaging Applications. Molecules. 2017;22(9):1445.
16. Simon J, Nampoori VPN, Kailasnath M. Facile synthesis of Au-Ag core shell and nanoalloy using femtosecond laser ablation and their optical characterization. Optik. 2019;195:163168.
17. Arvinte A, Crudu I-A, Doroftei F, Timpu D, Pinteala M. Electrochemical codeposition of silver-gold nanoparticles on CNT-based electrode and their performance in electrocatalysis of dopamine. J Electroanal Chem. 2018;829:184-193.
18. Khalil I, Julkapli N, Yehye W, Basirun W, Bhargava S. Graphene–Gold Nanoparticles Hybrid—Synthesis, Functionalization, and Application in a Electrochemical and Surface-Enhanced Raman Scattering Biosensor. Materials. 2016;9(6):406.
19. Patil MP, Kim G-D. Eco-friendly approach for nanoparticles synthesis and mechanism behind antibacterial activity of silver and anticancer activity of gold nanoparticles. Applied Microbiology and Biotechnology. 2016;101(1):79-92.

20. Menazea AA, Abdelghany AM. Precipitation of silver nanoparticle within silicate glassy matrix via Nd:YAG laser for biomedical applications. Radiat Phys Chem. 2020;174:108958.
21. Torrisi A, Cutroneo M, Torrisi L, Vacík J. Biocompatible nanoparticles production by pulsed laser ablation in liquids. Journal of Instrumentation. 2020;15(03):C03053-C03053.
22. Hmoad NR, Ali AH, Saadoon AM, Abdulkareem AA, Albayati AH. Effect of different wing geometries on their vibration characteristics. Frontiers in Mechanical Engineering. 2026;11.
23. Farhana N. Bio-Inspired Swarm-Transformer Hybrid Algorithm for HighPrecision Nanomaterial Design and Experimental Validation in Biomedical Applications. Ci-STEM Journal of Advanced Materials and Computing. 2026;01(01):09-16.
24. Jasim MN, Ahmed Kareem S. The Study of Optical and Structural Properties of NiO - SnO_2: CdO Nanostructures Thin Films. Iraqi Journal of Nanotechnology. 2022(3):11-19.
25. Rahmah MI, Saadoon NM, Mohasen AJ, Kamel RI, Fayad TA, Ibrahim NM. Double hydrothermal synthesis of iron oxide/silver oxide nanocomposites with antibacterial activity **. Journal of the Mechanical Behavior of Materials. 2021;30(1):207-212.